Available online at www.sciencedirect.com
ScienceDirect
Ultramicroscopy 108 (2008) 552–557
ultramicroscopy
www.elsevier.com/locate/ultramic

Planar patch-clamp force microscopy on living cells

Evren Pamir[a], Michael George[b], Niels Fertig[b], Martin Benoit[a,*]

[a]Center for Nano Science, Ludwig-Maximilians University, Amalienstr 54, 80799 Munich, Germany
[b]Nanion Technologies GmbH, Erzgiessereistr. 4, 80335 Munich, Germany

Received 17 April 2007; received in revised form 16 August 2007; accepted 29 August 2007

Abstract

Here we report a new combination of the patch-clamp technique with the atomic force microscope (AFM). A planar patch-clamp chip microstructured from borosilicate glass was used as a support for mechanical probing of living cells. The setup not only allows for immobilizing even a non-adherent cell for measurements of its mechanical properties, but also for simultaneously measuring the electrophysiological properties of a single cell. As a proof of principle experiment we measured the voltage-induced membrane movement of HEK293 and Jurkat cells in the whole-cell voltage clamp configuration. The results of these measurements are in good agreement with previous studies. By using the planar patch-clamp chip for immobilization, the AFM not only can image non-adhering cells, but also gets easily access to an electrophysiologically controlled cellular probe at low vibrational noise.

Keywords: AFM; Patch-clamp; Planar patch-clamp chip; Voltage-induced membrane movement; Immobilizing non-adherent cells; HEK293 cells; Jurkat cells

1. Introduction

Several studies have simultaneously investigated the electrical and the mechanical properties of living cells by combining the patch-clamp technique with the atomic force microscope (AFM) [1–6]. In modern electrophysiology, the patch-clamp technique has become a standard tool for the investigation of ion channels in cellular membranes [7–9]. Usually small glass pipettes are used for the electrical analysis or manipulation of the cell. For automated high throughput screening the concept of planar patch-clamp was developed recently [10]. On the other hand, the AFM [11] provides a standard method for mechanical probing of cells. For instance, indenting an AFM tip into a cell resting on a substrate allows to determine the cytoskeletal stiffness of a cell [12]. Especially for non-adherent cells such measurements require a suitable method for immobilizing the cell. The classical method consists in fixing the cell by bio-chemically crosslinking to the substrate (Fig. 1a). In principle, tethering spherical objects to a planar surface results to be difficult and some properties of the cell might be altered by the crosslinking [13]. Other approaches are microstructured substrates capable to cage and therefore to prevent lateral movements (Fig. 1b and 1c) [14,15]. Here we use a plane substrate with a single microstructured hole to immobilize a non-adherent spherical Jurkat cell. In combined patch-clamp–AFM measurements, different configurations between the patch-clamp pipette, the AFM tip and the probed cell have so far been realized (Fig. 1d and 1e). In this study we complement the set of possible configurations by combining the AFM with a planar patch-clamp chip (Fig. 1f). We employ planar microstructured borosilicate glass chips (Nanion Technologies GmbH, Munich, Germany), used in a commercially available patch-clamp workstation (Port-a-Patch from Nanion), which commonly is used for automated patch-clamp recording purposes alone [16,17]. The planar geometry of the chip is predestined for the combination with an AFM because immobilization and electrical analysis require only one contact point.

As an ideal proof of principle experiment for our setup, we measured the voltage-induced membrane movement of HEK293 cells and Jurkat cells. This effect has already been

*Corresponding author. Tel.: +49 89 2180 3133.
E-mail address: martin.benoit@physik.uni-muenchen.de (M. Benoit).

0304-3991/$ - see front matter © 2007 Elsevier B.V. All rights reserved.
doi:10.1016/j.ultramic.2007.08.013

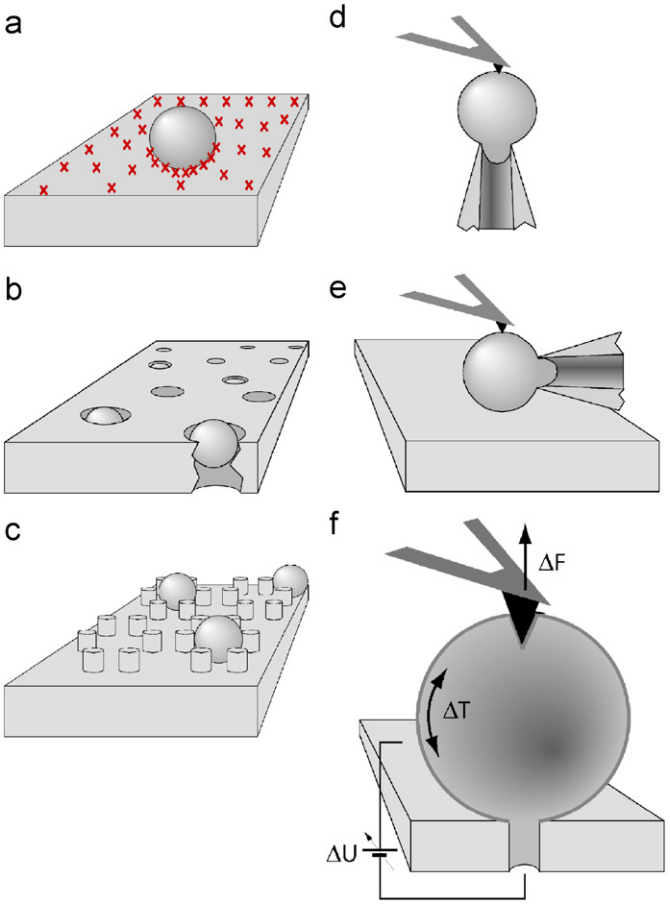

Fig. 1. Schematic drawings of possible immobilization strategies for probing living cells with an AFM. (a) Bio-chemically tethering of the cell to the substrate. (b) Caging the cells in holes of the cell size. (c) Caging the cells in posts. (d) The cell is fixed in a patch-clamp pipette while being mechanical probed. The axis of rotational symmetry is confined by the cantilever tip and the aperture of the pipette (as in (f) too). (e) The cell is laterally accessed by a patch-clamp pipette while resting on a substrate. (f) Configuration of our setup. The cell is immobilized and electrically accessed by the patch-clamp hole of the planar patch-clamp chip while mechanically probed by the AFM tip. The abbreviations illustrate the voltage-induced membrane movement described in Section 1: A change of transmembrane voltage ΔU (V) causes a change of the mechanical membrane tension ΔT (N/m) which produces a normal force ΔF (N) on an indented AFM tip.

explained and demonstrated in great detail by Zhang et al. [2] using HEK293 cells as a model system. Briefly, modifying the transmembrane voltage of a voltage-clamped cell in whole-cell mode causes a change of mechanical membrane tension which can be detected by an AFM tip indenting the cell (Fig. 1f). The change of mechanical membrane tension is explained by the Lippman equation, a thermodynamic principle, which relates interfacial tension to electrostatic potential. By applying the Lippman equation to the extra- and intracellular side of the membrane a quantitative expression is obtained for the change of mechanical membrane tension ΔT (N/m) dependent on the change of transmembrane ΔU (V) voltage. A normal force ΔF (N) displacing the AFM cantilever is derived when considering the geometric configuration between the cell membrane and the indented AFM tip. The experimental key features of the voltage-induced membrane movement are as follows. (i) In physiological ionic strength extracellular solution, depolarization of the membrane causes an outward movement of the cantilever and in low ionic strength solutions the displacement of the cantilever reverts. (ii) In good approximation, the amplitude of the displacement will be proportional to the applied transmembrane voltage change, in the range of −180 to 0 mV of the applied holding potential. (iii) The amplitude of the displacement increases with the indentation force of the cantilever and assuming Hertzian mechanics the displacement should be dependent on the square root of the indentation force. (For more detail see Ref. [2].)

2. Materials and methods

Our experimental setup consists of three major units: the homebuilt force spectrometer, the patch-clamp device and the inverted optical microscope (Figs. 2 and 3). The homebuilt force spectrometer could be easily replaced by a commercial scanning force microscope (Bioscope, Digital Instruments, Santa Barbara, USA). For the patch-clamp instrumentation we used the Port-a-Patch workstation (Nanion Technologies GmbH, Munich, Germany) [10]. The construction of a new chip support allowed the integration of the inverted optical microscope (20 × Long Distance, Epiplan, Zeiss, Germany) and a CCD camera (I-cam, Apple Inc., Cupertino, USA). Optionally, we used a patch-clamp pipette for the positioning of a cell on the patch-clamp aperture. Control and data acquisition of the measurements were done with Igor Pro (Wavemetrics, Portland, USA). The data shown are lowpass filtered at 2 kHz.

Extracellular solution (on the upper surface of the patch-clamp chip) contained (in mM): 160 NaCl, 4.5 KCl, 1 $MgCl_2$, 2 $CaCl_2$, 5 C-glucose monohydrate, 10 Hepes/NaOH pH 7.4 (referred as physiological ionic strength). Intracellular solution (on the lower side of the chip) contained (in mM): 75 KCl, 10 NaCl, 70 K-fluoride, 2 $MgCl_2$, 10 EGTA, 10 Hepes/KOH, pH 7.2.

HEK and Jurkat cells were maintained in RPMI-1640 medium (Biochrom AG) supplemented with 10% heat-inactivated FCS, 2 mM L-glutamine and penicillin/streptomycin in 5% CO_2 at 37 °C. Before the measurements, cells were washed with 5 mM EDTA and re-suspended in extracellular solution. A few picoliter of a solution of 10^6 cells/ml was injected close to the aperture acting as a sink at −10 mbar pressure After the resistance of the aperture indicated a cell attached by raising to some 10 MΩ, the floating cells were gently washed away with extracellular solution.

Then either AFM images were taken at room temperature with the Bioscope in constant deflection mode (at lowest possible setpoint of 0.1 V an integral gain of 3 and 1 Hz scan rate) on a Jurkat cell in cell-attached mode or the

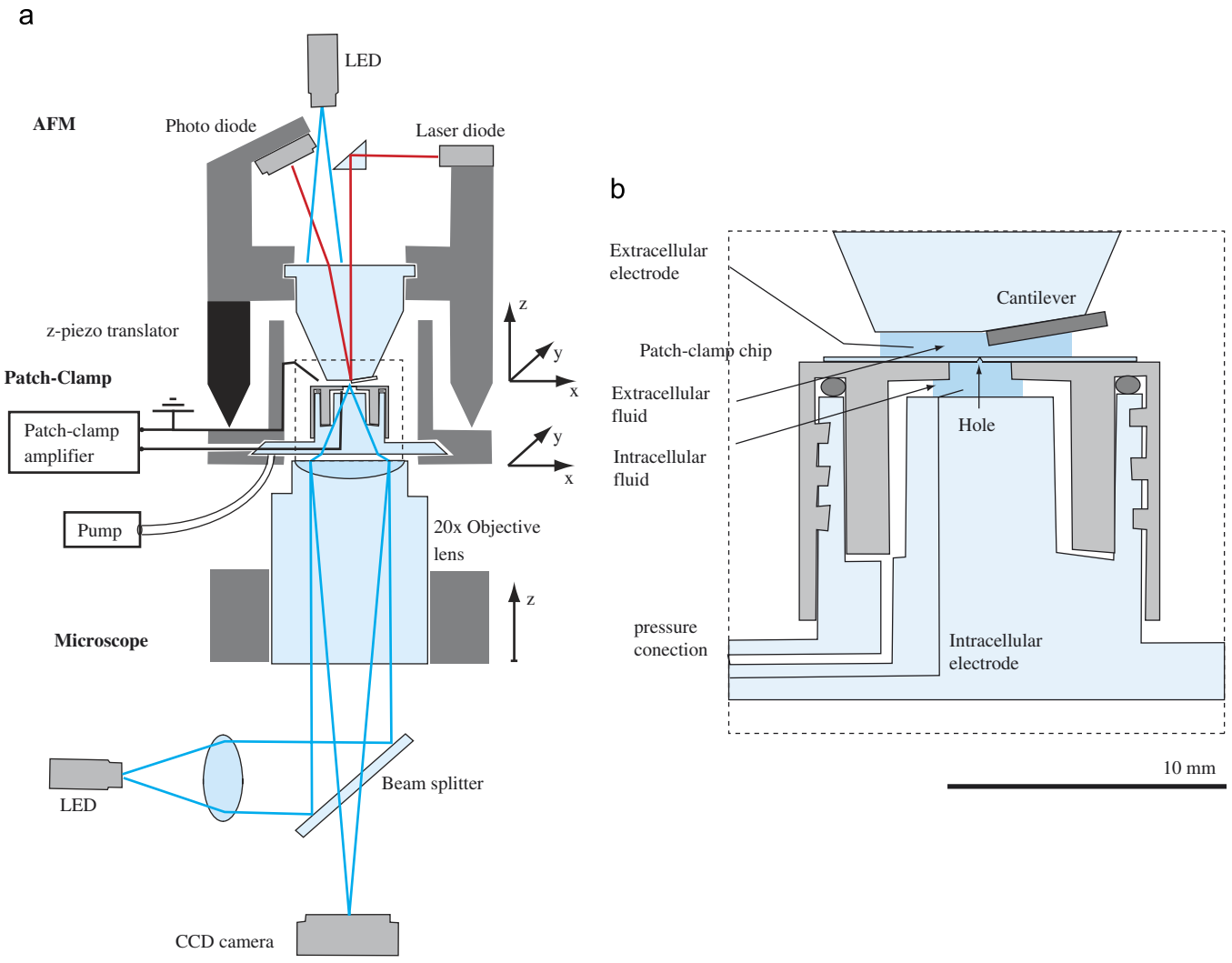

Fig. 2. (a) The experimental setup consists of three major units: the AFM (with the z-piezo and the laser detection system), the patch-clamp device (with two electrodes connected to the patch-clamp amplifier and suction unit) and the optical microscope (with the illumination and camera). (b) Expanded view of the core unit. The cell to be measured is located on top of the aperture in the droplet formed between the Cantilever holder and the planar patch-clamp chip at ambient pressure. The droplet bears the extracellular electrode (Ag/AgCl) and the cantilever. The AFM tip is precisely brought into contact to the cell at a defined force. The droplet below the aperture at tunable pressure between ± 250 mbar is contacted to the intracellular electrode (Ag/AgCl).

combined patch-clamp AFM measurements were performed at room temperature with whole-cell voltage-clamped HEK293 and Jurkat cells while maintaining a gigaseal. The patch-clamp chips had an aperture of $2.5 \pm 0.5\,\mu$m leading to an open chip resistance of about 2–3 MΩ. The homebuilt force spectrometer (Fig. 3) was placed on top of the patch-clamp chip and controlled by modified software and hardware originated from Asylum-Research (Santa Barbara, USA). The mechanical probing of the cells was done with microfabricated, pyramid-shaped, silicon nitride AFM cantilever tips (lever C, gold-coated, spring constant 18 ± 3 pN/nm, Park Scientific, Sunnyvale, USA).

3. Results

As a proof of principle experiment for our setup, we measured the voltage-induced membrane movement of HEK293 and Jurkat cells. In a set of experiments, both cellular systems showed the experimental key features (i, ii, iii) described in Section 1. Fig. 4 shows the experimental data from one experiment with a whole-cell voltage-clamped HEK293 cell. The cell was indented several times at different indentation forces ($N = 20$). During indentation, a pulse protocol changing the transmembrane voltage was applied (Fig. 4b). This change of transmembrane voltage caused a normal force on the cantilever, which was detected as a displacement in the deflection signal (Fig. 4a). At a given indentation force, hyperpolarizing the cell membrane by -20 mV caused an inward movement of the cantilever to the cell and subsequently depolarizing by $+100$ mV caused an outward movement. The amplitude of these displacements increased with the indentation force (Fig. 4c). Fitting a simple square root function (drawn through lines) to the displacements shows good agreement with the underlying model involving Hertzian mechanics

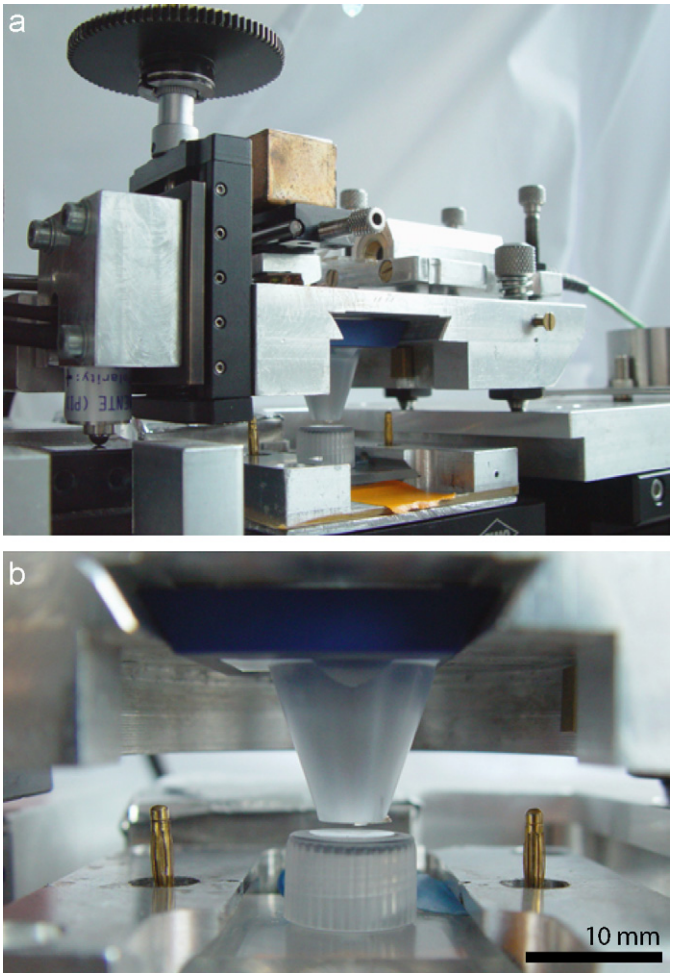

Fig. 3. (a) Picture of the experimental setup showing the homebuilt AFM mounted onto the modified patch-clamp device. (The Faraday cage has been removed.) (b) Enlarged view of the experimental chamber showing the cantilever holder accessing the patch-clamp chip surface.

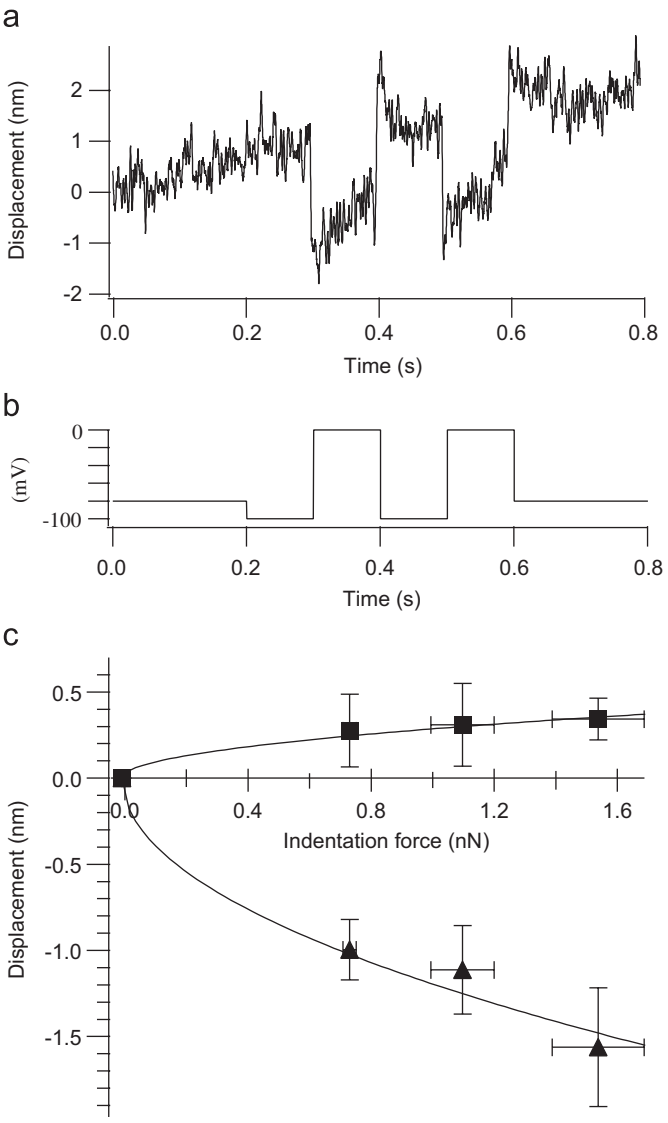

Fig. 4. Voltage-induced membrane movements of HEK293 cells at physiological ionic strength. (a) Deflection signal of the cantilever resting on the cell membrane at an indenting force of 1.5 nN. A decreasing deflection signal corresponds to the cantilever moving towards the cell exterior. (b) Applying hyperpolarizing (−20 mV) and depolarizing (+100 mV) voltage steps leads to corresponding displacements of the cantilever. (c) Displacements of the cantilever caused by −20 mV voltage changes (quadrangle) and +100 mV voltage changes (triangle) versus the applied indentation force of the cantilever. The data points coincide with previous findings, stating that the displacements are a function of the square root of the indentation force (drawn through lines from a numerical square root fit to the data).

set up by Zhang et al. Taking the ratio between the displacements caused by depolarizing (+100 mV) and hyperpolarizing (−20 mV) leads to a value of (3.9±09). This value approximately reflects the proportionality between the applied voltage change and the cantilever displacement. However, we did not perform experiments over the full range of extracellular ionic concentrations which is necessary for estimating the extra- and intracellular charge densities of the probed membranes. To compare our results in quantitative terms with the results from Zhang et al.: at an indentation force of 1.0 nN we observed a displacement of 1.1±0.4 nm which corresponded to a +100 mV voltage change (Zhang et al.: 0.8 nm).

Upon lowering the extracellular ionic concentration (<5 mM), the reversal of the cantilever displacements was observed (traces not shown).

The experiments concerning the voltage-induced membrane movement of Jurkat cells led to similar results (Fig. 5). On average, Jurkat cells showed higher displacements of the cantilever (1.9±0.4 nm/100 mV at 1.0 nN; $N = 40$) in comparison to HEK293 cells. Jurkat cells endogenously express voltage-gated potassium channels (Kv1.3) in their membrane, therefore we simultaneously could record the whole-cell current during indentation (Fig. 5c). While depolarizing the membrane, apart from the corresponding displacement of the cantilever (Fig. 5a) the characteristic current pattern for the Kv1.3 activation was observed. These measurements on Jurkat cells thereby show that the planar patch-clamp chip provides a suitable

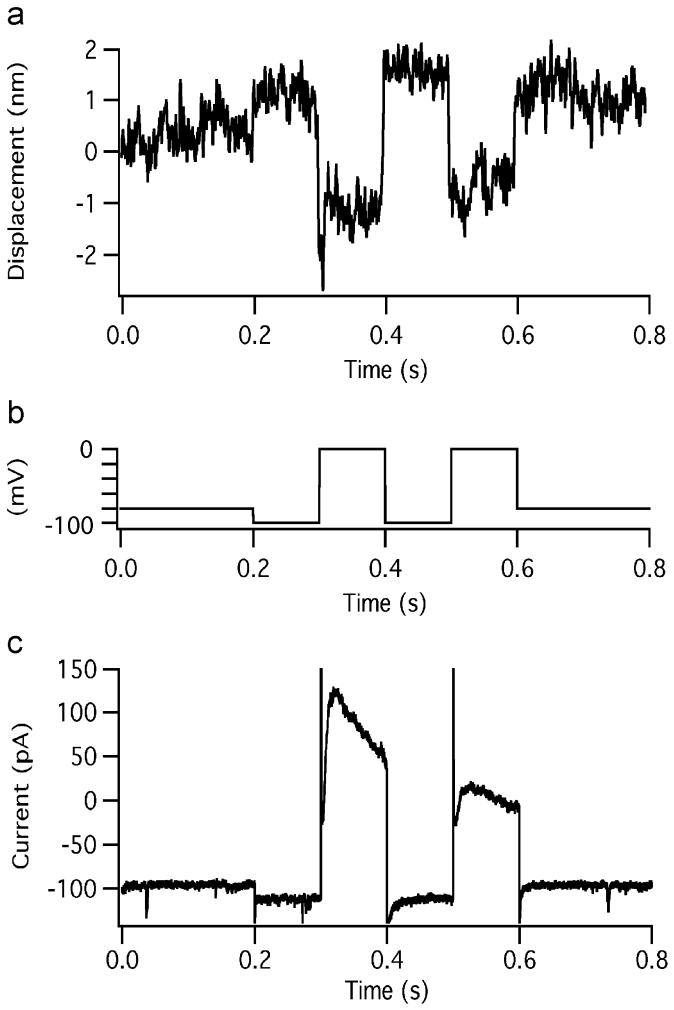

Fig. 5. Voltage-induced membrane movements of a Jurkat cell at physiological ionic strength. (a) Deflection signal of the cantilever resting on the cell membrane at an indenting force of 1.0 nN. (b) Applied pulse protocol which causes corresponding cantilever displacements. (c) Corresponding whole-cell current. Upon depolarization of the membrane, the characteristic response of the voltage gated potassium channel Kv1.3 in Jurkat cells is observed.

immobilization tool for both the mechanical and the electrophysiological probing of non-adherent cells.

Although the linkage between the patch-clamp aperture and the cell membrane is rather fragile compared to a firmly attached cell spread on a surface, mechanical probing of the cell can be done while maintaining the gigaohm seal (a prerequisite for high quality electrophysiological recordings of ionic currents without leak current). Due to the rotational symmetry of our configuration (see Fig. 1f), no shear forces are acting on the seal under mechanical load from force spectroscopy measurements. Even for AFM imaging of the rather soft Jurkat cells in scanning mode the immobilization was stable enough if the normal force is set to the lowest and the feedback loop to the highest level (Fig. 6). Although the AFM image has no scientific relevance for the Jurkat cells, it can serve as a proof for the immobilization efficiency. If

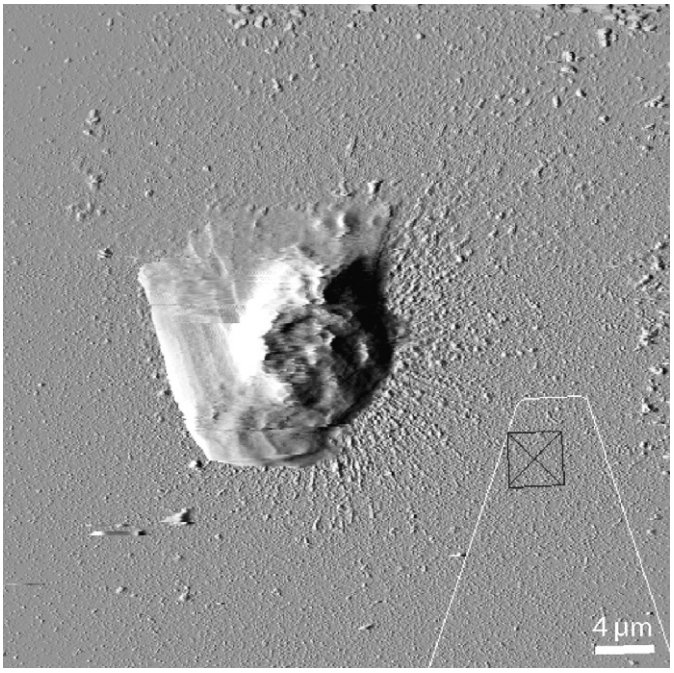

Fig. 6. AFM deflection image of an immobilized Jurkat cell on the patch-clamp chip (setpoint below 50 pN). The schematic drawing indicates the geometry and orientation of the cantilever generating this image. The cell is attached to the patch-clamp chip by a suction pressure of 20 mbar.

the cell surmounts the height of the tip, the triangular shape of the cantilever becomes visible in the vicinity of the cell. Since the geometry of the pyramidal tip ($4 \times 4 \times 4\,\mu m^3$) was in the order of the object (cell radius 5 µm) not only the tip images the object but the object even probes the cantilever structure. The drawn-to-scale scheme of the cantilever used for these images is shown in Fig. 6 as well.

4. Discussion

Mechanical methods to immobilize cells for AFM access, which do not include the electrophysiological analysis, have been established in previous studies with non-adherent cells [15,18,19].

Combining the patch-clamp technique with the AFM is a challenging experimental procedure and no standard method has so far been established for this purpose. Choosing the right instrumentation crucially depends on the properties of the cellular system, which is to be investigated. By combination of a standard planar patch-clamp workstation and a custom built AFM, we were able to construct a platform ideally suited for concomitant electrophysiological characterization/manipulation and AFM probing of a single cell. In principle, the optical microscope can be integrated to the setup either from above or from below the patch-clamp chip plane. Choosing the variant from below allowed us to view and access the chip surface during all stages of the performed experiment, which is of great advantage for the experimenter. Alternatively, the microscope could be mounted on top of the

setup in a manner realized in a previous study [3] using patch-clamp pipettes in combination with the AFM. For this approach, the commercial Port-a-Patch workstation could be used without the need to construct a special chip support.

The Jurkat cells showed a two-fold larger voltage-induced membrane displacement compared to HEK293 cells. This discrepancy might be a hint for the Jurkat cells have some significant differences in the arrangement of their membrane compared to the HEK cells. Guided from their elastic response, when indenting the cells, we believe that the anchorage of the Jurkat cell membrane to the cytoskeleton is weaker and therefore might allow for larger voltage-induced movements of the membrane. Combining patch-clamp and force-spectroscopy might turn out to be a powerful tool to characterize not only ionic but also mechanical properties of the membrane, its constituents and its linkage to the cytoskeleton, which will be subject for further investigation.

Imaging non-adherent cells on this setup—though possible—does not gain good resolution on soft samples like the Jurkat cells. Nevertheless, the immobilization is sufficient and fundamental for force spectroscopy experiments. We even assume that the compact planar chip as a substrate might reduce the vibrational noise compared to a conventional thin and long patch-clamp pipette mounted to a micromanipulator unit.

The combined setup enables measurement of two parameters simultaneously: the electrophysiological and the mechanical properties of the cell responding to a stimulus. Either of the parameters can be used for stimulation or read out, respectively.

A particular interesting cellular system for our setup may turn out to become cell cultures [20] expressing the motor protein Prestin [21]. This molecular motor from the hair cells of the inner ear is evenly distributed in the cellular membrane of genetically transfected cells. A symmetric probing configuration as provided by our setup may be of great advantage for thorough analysis of the characteristics of that motor protein.

Acknowledgments

This work was partially founded by the ProInno program (AiW, Germany), the DFG and Nanion Technologies GmbH. This work was not possible without the electro-technical knowledge of Stephan Manus and Christian Holopirek. We especially thank Angelika Kardinal and Thomas Nicolaus for the cell culture as well as Andrea Brüggemann and Sonja Stölze for the introduction into planar patch-clamp.

References

[1] J.K. Hörber, J. Mosbacher, W. Häberle, J.P. Ruppersberg, B. Sakmann, Biophys. J. 68 (1995) 1687.
[2] P.C. Zhang, A.M. Keleshian, F. Sachs, Nature 413 (2001) 428.
[3] M.G. Langer, W. Offner, H. Wittmann, H. Flosser, H. Schaar, W. Haberle, A. Pralle, J.P. Ruppersberg, J.K.H. Horber, Rev. Sci. Instrum. 68 (1997) 2583.
[4] J. Mosbacher, M. Langer, J.K. Hörber, F. Sachs, J. Gen. Physiol. 111 (1998) 65.
[5] M.G. Langer, A. Koitschev, H. Haase, U. Rexhausen, J.K. Hörber, J.P. Ruppersberg, Ultramicroscopy 82 (2000) 269.
[6] M.G. Langer, S. Fink, A. Koitschev, U. Rexhausen, J.K. Hörber, J.P. Ruppersberg, Biophys. J. 80 (2001) 2608.
[7] E. Neher, B. Sakmann, Nature 260 (1976) 799.
[8] K.S. Cole, Annu. Rev. Physiol. 41 (1979) 1.
[9] E. Neher, B. Sakmann, Proc. Natl. Acad. Sci. USA 72 (1975) 2140.
[10] A. Brueggemann, M. George, M. Klau, M. Beckler, J. Steindl, J.C. Behrends, N. Fertig, Curr. Drug Discov. Technol. 1 (2004) 91.
[11] G. Binnig, C.F. Quate, C. Gerber, Phys. Rev. Lett. 56 (1986) 930.
[12] C. Rotsch, M. Radmacher, Biophys. J. 78 (2000) 520.
[13] A.J. Engler, S. Sen, H.L. Sweeney, D.E. Discher, Cell 126 (2006) 677.
[14] T.W. Holstein, M. Benoit, G.v. Herder, G. Wanner, C.N. David, H.E. Gaub, Science 265 (1994) 402.
[15] M.J. Rosenbluth, W.A. Lam, D.A. Fletcher, Biophys. J. 90 (2006) 2994.
[16] N. Fertig, R.H. Blick, J.C. Behrends, Biophys. J. 82 (2002) 3056.
[17] A. Bruggemann, S. Stoelzle, M. George, J.C. Behrends, N. Fertig, Small 2 (2006) 840.
[18] M. Benoit, T. Holstein, H.E. Gaub, Eur. Biophys. J. 26 (1997) 283.
[19] S. Kasas, A. Ikai, Biophys. J. 68 (1995) 1678.
[20] K. Iida, K. Tsumoto, K. Ikeda, I. Kumagai, T. Kobayashi, H. Wada, Hear Res. 205 (2005) 262.
[21] J. Zheng, L.D. Madison, D. Oliver, B. Fakler, P. Dallos, Audiol. Neurootol. 7 (2002) 9.